The Cosmic Microwave Background/Le rayonnement fossile à 3K

Archeops results

Jean-Christophe Hamilton [a,b,c,*], Alain Benoit [d], the Archeops collaboration [1]

[a] *LPNHE (CNRS-IN2P3), Paris VI & VII, 4, place Jussieu, 75252 Paris cedex 05, France*
[b] *LPSC (CNRS-IN2P3), 53, avenue des Martyrs, 38026 Grenoble cedex, France*
[c] *PCC (CNRS-IN2P3), 11, place Marcelon Berthelot, 75231 Paris cedex 05, France*
[d] *CRTBT (CNRS), 25, avenue des Martyrs, BP 166, 38042 Grenoble cedex 9, France*

Presented by Guy Laval

Abstract

Archeops is a balloon-borne instrument, dedicated to measuring cosmic microwave background (CMB) temperature anisotropies at high angular resolution (∼12 arcmin.) over a large fraction (30%) of the sky in the (sub)millimetre domain (from 143 to 545 GHz). We describe the results obtained during the last flight: the Archeops estimate of the CMB angular power spectrum, linking for the first time Cobe scales and the first acoustic peak, consequences in terms of cosmological parameters favouring a flat-Λ Universe. We also present the first measurement of galactic dust polarization and accurate maps of the galactic plane diffuse (sub) millimetre emisson. ***To cite this article: J.-C. Hamilton et al., C. R. Physique 4 (2003).***
© 2003 Académie des sciences. Published by Elsevier SAS. All rights reserved.

Résumé

Expérience Archeops. Archeops est une expérience ballon destinée à mesurer les anisotropies du fond diffus cosmologique (CMB) avec une haute résolution angulaire (∼12 arcmin.) sur une large fraction du ciel (30%) dans le domaine (sub)millimetrique (de 143 à 545 GHz). Nous décrivons les résultats obtenus durant le dernier vol : la mesure du spectre de puissance angulaire des anisotropies du CMB reliant pour la première fois les échelles de Cobe avec le premier pic acoustique, les conséquences en termes de paramètres cosmologiques qui favorisent un Univers plat dominé par une constante cosmologique. Nous présentons aussi la première détection de polarisation des poussières galactiques ainsi que des cartes précises de l'émission diffuse (sub)millimetrique du plan galactique. ***Pour citer cet article : J.-C. Hamilton et al., C. R. Physique 4 (2003).***
© 2003 Académie des sciences. Published by Elsevier SAS. All rights reserved.

Keywords: Cosmic Microwave Background anisotropies; Cosmology; Early Universe

Mots-clés : Anisotropies du fond de rayonnement cosmique ; Cosmologie ; Univers primordial

1. Introduction

The Cosmic Microwave Background (CMB) gives many clues as to the origin of the Universe. It contains a wealth of diverse information, in contrast with the other 2 so-called pillars of Cosmology. The advent of BLIP (Background limited Performance) detectors (bolometers at 100 to 300 mK) and mostly sidelobe-free HEMT based interferometers has provided CMB maps with increasing accuracy and resolution in the last 10 years. The fluctuations that are now routinely detected in a

---

few hours-days of integration time (e.g., [1–7]) provide vivid proof of the seeds that lead to large-scale structure formation. They are best analysed with the spherical harmonic angular power spectrum C_ℓ as a function of the multipole ℓ familiar to quantum physics. The generation of the power spectrum is now theoretically understood so that cosmological parameters can be deduced accurately. Archeops [2] is a CMB bolometer-based instrument with Planck–Hfi[3] technology that fills a niche where previous experiments were unable to provide strong constraints. Namely, Archeops seeks to join the gap in ℓ between the large angular scales as measured by Cobe/Dmr and degree-scale experiments, typically for ℓ between 10 and 200. For that purpose, a large sky coverage is needed. The solution was to adopt a spinning payload mostly above the atmosphere, scanning the sky in circles with an elevation of around 41 degrees. The Earth's rotation makes the circle span a large area of the sky.

In Section 2 we will describe the instrument characteristics and the various flights, in Section 3 the data analysis process. We will present the results concerning the CMB angular power spectrum in Section 4 and the cosmological constraints in Section 5. The Archeops diffuse galactic emission maps is presented in Section 6 and the first detection of galactic dust polarization will be presented in Section 7.

2. Instrument and flights

The instrument [8] was designed by adapting concepts put forward for Planck–Hfi and using balloon-borne constraints: namely, an open ^{3}He–^{4}He dilution cryostat cooling spiderweb-type bolometers at 100 mK, cold individual optics with horns at the different temperature stages (0.1, 1.6, 10 K) and the telescope. The Gregorian off-axis aluminum telescope is made of an effective 1.5 m aperture primary and a secondary ellipsoid mirror. The whole instrument is baffled so as to avoid stray radiation from the Earth and the balloon. The scan strategy imposes an observation by night. Maximising integration time means going above the Arctic circle. After a test flight in Trapani (Sicily) with four-hours integration time, the upgraded instrument was launched three times from the Esrange base near Kiruna (Sweden) by the CNES in the last two Winter seasons. The last and best flight on 7 February 2002 yields 12.5 hours of CMB-type data (at ceiling altitude and by night) from a 19 hours total. The balloon landed in Siberia and it was recovered (with its precious data recorded on-board) by a Franco–Russian team with -40 deg·C·weather.

3. Data analysis

The data are calibrated with the CMB dipole [9], the FIRAS Galaxy and Jupiter (point-like) emission (beside yielding effective beams of typically 12 arcminute FWHM). The calibration error on the dipole is estimated as 4% and 8% at 143 and 217 GHz, respectively. The other methods have calibration uncertainties of about 10% and are consistent with the dipole calibration within less than 20%. Eight detectors at 143 and 217 GHz are found to have a sensitivity better than 200 μK_{CMB} rms, in one second of integration corresponding to the stationary part of the noise. For a square pixel of 20 arcmin the average 1σ sensitivity with all detectors combined per channel is 100 and 150 μK_{CMB} (0.04 and 0.06 MJy/sr) at 143 and 217 GHz, respectively. It is 0.4 and 0.8 MJy/sr at 353 and 545 GHz. A large part of the data reduction was devoted to removing additional noise which comes from the various thermal stages at frequencies $f \leqslant 0.03$ Hz, and atmospheric effects: an elevation systematic effect is seen below 0.1 Hz and the four frequencies are correlated between 0.1 and 1 Hz. These decorrelations in the timelines are mostly done for the low $\ell < 30$ side of the power spectrum. The data are cleaned and calibrated, and the pointing is reconstructed from stellar sensor data [10].

We then make CMB-designed maps in the cleanest region (from the Galactic foreground point of view) restricted to $b > +30$ deg. giving a total of $\sim 10^5$ 13.7 arcmin. pixels (HEALPIX nside = 256) covering 12.6% of the sky (see Fig. 1). The maps are obtained by coadding filtered data (bandpass between 0.3 and 45 Hz) avoiding ringing effects with a process described in [12]. Residual ringing is estimated to be less than $\sim 36 \mu K^2$ on the power spectrum in the first ℓ-bin and negligible for larger multipole. We then only keep maps of two best photometers, one at 143 GHz and one at 217 GHz which are coadded using a $1/\sigma^2$ weighting (σ being the noise RMS in each pixel). We apply the MASTER method [13] to estimate the CMB power spectrum from these maps. The noise Fourier power spectrum is estimated from the time stream data using the algorithm described in [12]. Our maps show structure on the sky at the degree angular scale that can be attributed to CMB anisotropies. A comparison of the anisotropies seen by Archeops and by WMAP is shown in Fig. 2.
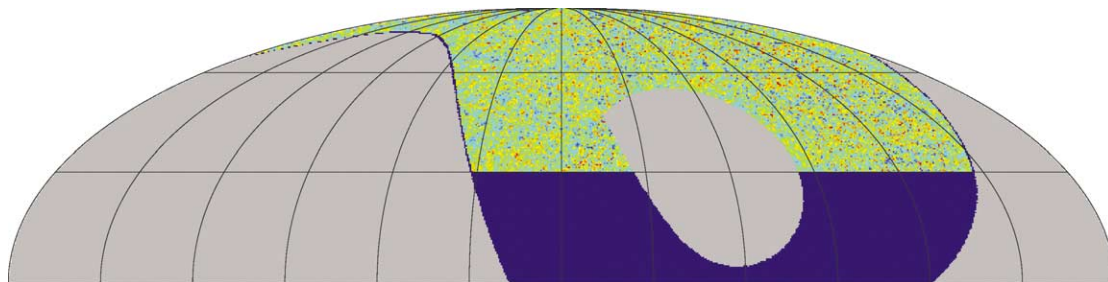

Fig. 1. Archeops CMB map (Galactic coordinates, north hemisphere) in HEALPIX pixelisation [11] with 13.7 arcminutes pixels and a 15 arcminutes Gaussian smoothing. The map was made by coadding the data from 2 photometers as discussed in the text. The dark blue region is not included in the present analysis because of possible contamination by dust. The Galactic anticenter is at the center of the map. The colors in the map range from -500 to 500 μK_{CMB}.

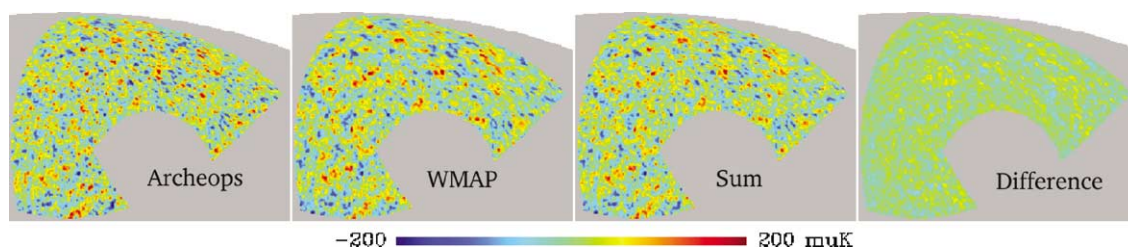Fig. 2. Comparison of the Archeops and WMAP datasets. The first map is from Archeops (convolved with a Gaussian beam of FWHM = 1 deg. and rotated to help visualisation). The second map is the same part of the sky from WMAP [14]. It is also convolved to a 1 deg·FWHM and large scales not present in the Archeops map are removed by subtracting the WMAP map convolved to a 15 deg·FWHM·map. The third and fourth maps show the half sum and half difference, both are performed without any intercalibration. The strong correlation between both datasets is obvious.

4. Angular power spectrum results

The CMB anglar power spectrum is estimated in 16 bins ranging from $\ell = 15$ to $\ell = 350$ (see Table 1, and Fig. 3 for a comparison with a selection of other recent experiments and a best-fit theoretical model). Much attention was paid to the possible systematic effects that could affect the results. At low ℓ, dust contamination and at large ℓ, bolometer time constant and beam uncertainties are all found to be negligible with respect to statistical error bars. The sample variance at low ℓ and the photon noise at high ℓ are found to be a large fraction of the final Archeops error bars in Fig. 3. Various tests for systematic effects have been performed, such as Jack-knife tests and are described in [15].

The first acoustic peak appears clearly from Archeops data itself. A Gaussian fit of the Archeops and the COBE data leads to a location of the peak at $\ell_{peak} = 220 \pm 6$ with a width $FWHM = 192 \pm 12$ and an amplitude $\delta T = 71.5 \pm 2.0$ μK, compatible with previous determinations and achieving a better precision than earlier experiments, even combined together. One of the main goals of the experiment, i.e., to provide an accurate link between the large angular scales from Cobe and the first acoustic peak as measured by degree-scale experiments such as Boomerang, Cbi, Dasi, Maxima, Vsa, has been achieved.

5. Cosmological constraints

Cosmological constraints can be placed on adiabatic cold dark matter models with passive power-law initial fluctuations. Because the Archeops power spectrum has small bins in ℓ and large ℓ coverage down to Cobe scales, it provides a precise determination of the first acoustic peak in terms of position at the multipole $l_{peak} = 220 \pm 6$, height and width. Using a large grid of cosmological adiabatic inflationary models described by 7 parameters, one can compute their likelihood with respect to the datasets. An analysis of Archeops data in combination with other CMB datasets constrains the baryon content of the Universe to a value $\Omega_b h^2 = 0.022^{+0.003}_{-0.004}$ which is compatible with Big-Bang nucleosynthesis (O'Meara et al. [16]) and with a similar accuracy (Fig. 4). Using the recent HST determination of the Hubble constant [17] leads to tight constraints on the total density, e.g., $\Omega_{tot} = 1.00^{+0.03}_{-0.02}$, i.e., the Universe is flat. An excellent absolute calibration consistency is found between Cobe, Archeops and other CMB experiments (Fig. 3). Finally, an analysis adding data from other CMB experiments (Cobe,

Table 1
The Archeops CMB power spectrum for the best two photometers (third column). The error bars are given at 1σ. Data points given in this table correspond to the red points in Fig. 3

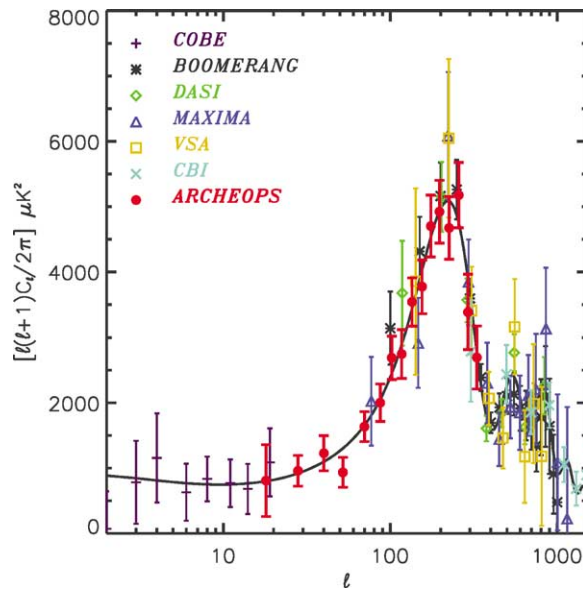| $\ell_{\min}$	$\ell_{\max}$	$\frac{\ell(\ell+1)C_\ell}{2\pi}$ $(\mu K)^2$
15	22	789 ± 537
22	35	936 ± 230
35	45	1198 ± 262
45	60	912 ± 224
60	80	1596 ± 224
80	95	1954 ± 280
95	110	2625 ± 325
110	125	2681 ± 364
125	145	3454 ± 358
145	165	3681 ± 396
165	185	4586 ± 462
185	210	4801 ± 469
210	240	4559 ± 467
240	275	5049 ± 488
275	310	3307 ± 560
310	350	2629 ± 471

Fig. 3. The Archeops CMB power spectrum from Table 1, compared to other degree-scale experiments.

Boomerang, Dasi, Maxima, Vsa and Cbi), the HST prior and an additionnal prior on the value of σ_8 (see [18] for details) leads to tight constraints on the quintessence parameters: $\Omega_Q = 0.70^{+0.10}_{-0.17}$ and $w_Q = -1^{+0.25}$ (95% CL) comforting the flat-Λ cosmological model.

All these measurements are fully compatible with inflation-motivated cosmological models. In particular, the best fit model shown in Fig. 3 is close to the mean likelihood Universe characterised by $\Omega_{\text{tot}} = 1.00^{+0.03}_{-0.02}$, $\Omega_\Lambda = 0.72^{+0.08}_{-0.06}$, $\Omega_b h^2 = 0.021^{+0.001}_{-0.003}$, $h = 0.69^{+0.06}_{-0.06}$, $n = 0.96^{+0.02}_{-0.04}$, $Q = 19.2$ µK, $\tau = 0$, obtained with Archeops and other CMB experiments and with the HST and $\tau = 0$ priors. Moreover, the constraints shown in Fig. 4 (right), leading to a value of $\Omega_\Lambda = 0.73^{+0.09}_{-0.07}$ for the dark energy content, is independent from and in agreement with supernovæ measurements [19] if a flat Universe is assumed.
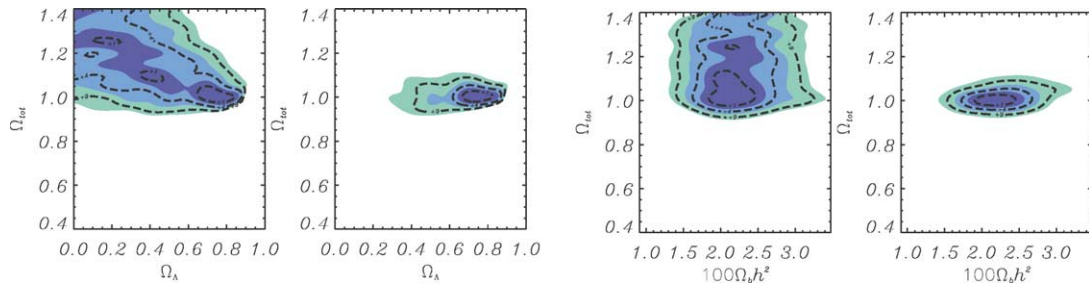
Fig. 4. Likelihood contours between 3 of the cosmological parameters: baryonic density and cosmological constant in the abscissae and total density as the ordinate. Greyscale corresponds to 2-D limits and dashed line to 1-D contours with the Gaussian equivalent of 1, 2, and 3σ thresholds. On the left, only the constraints from Archeops and other CMB experiments, identical to those in Fig. 3, are used. On the right panels, adding the prior on the Hubble constant $H_0 = 72 \pm 8$ km/s/Mpc (68% CL, Freedman et al. [17]) reduces significantly the allowed values of the cosmological parameters.
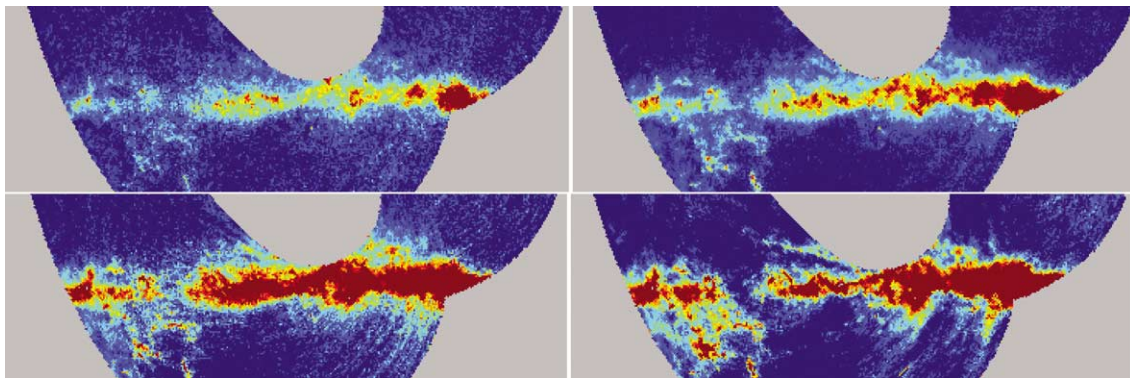

Fig. 5. Archeops Galactic maps at 143 GHz (top-left), 217 GHz (top-right), 353 GHz (bottom-left) and 545 GHz (bottom-right). The four maps are shown between 0 and 1 mK$_{\mathrm{RJ}}$.

6. Diffuse galactic plane emission maps

A specific data analysis pipeline has been designed to optimize the maps in the Galactic plane region. We use a destriping method that estimates the low frequency drifts by minimizing the cross-scan variations in the map and introduces a $2f_{\mathrm{spin}}$ highpass filter. The maps obtained by coadding all bolometers at each channel are shown in Fig. 5. These maps are the first Galactic plane high resolution maps at these frequencies on such a wide area of the sky. They show new dense bright regions, such as in the Taurus complex, on the lower-left part and also diffuse emission at large Galactic latitude.

7. Dust polarisation detection

The six 353 GHz Archeops channels are three Ortho Mode Transducers (hereafter OMT) [20,21] composed of a pair of bolometers having a common entry horn; the light is separated into its two linear polarizations with a polarizer beam splitter, one polarization is transmitted to the first bolometer and the second one reflected to the second bolometer. The sum of two coupled bolometers measures the total intensity while their difference measures the Q Stokes parameters in the OMTs eigen basis. The three OMT are oriented at 60 degrees from each other following the recommendations of [22] to optimize the polarization reconstruction. Details on the Archeops polarization experimental setup and data analysis will be found in [23].

A specific analysis pipeline is used for the polarisation analysis. Cross-calibration between two coupled channels is obtained by intercomparing the large signal coming from Galactic latitude profiles from different bolometers. Simulations show that the method leads to an accuracy on the cross-calibration better than 1% which is sufficient to measure galactic dust polarization in an unbiased way. The time stream data are filtered using a combination of the method described in [12], used for the Archeops CMB analysis and wavelet shrinkage techniques [24]. This ensures that no ringing is created in the Galactic plane region. The filtered polarization channels are then combined to produce maps of I, Q and U with a pixel size of 27.5 arcmin. (HEALPIX nside = 128). The maps are clipped to remove pixels containing less than 100 time samples corresponding to a
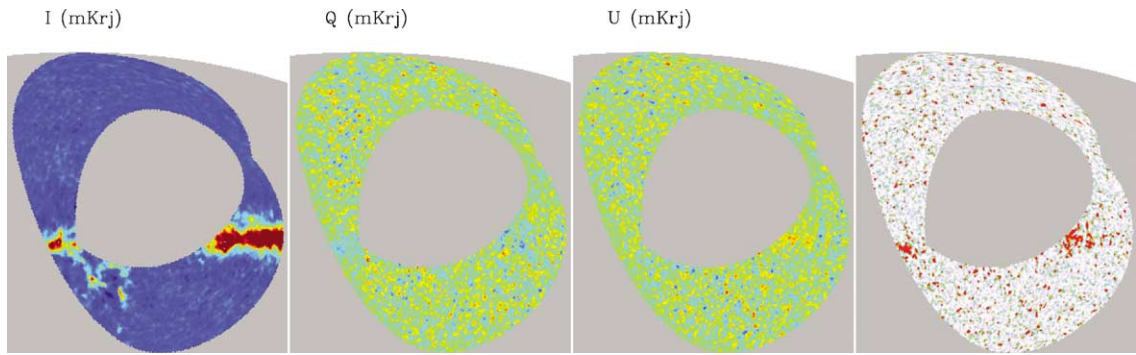
Fig. 6. Archeops I, Q, U and normalized squared polarized intensity maps (from left to right). The color scales ranges are $[-2, 1]$ mK$_{RJ}$ for the I map, $[-2, 2]$ mK$_{RJ}$ for the Q and U maps and $[0, 4]$ for the normalized squared polarized intensity map. In the latter map, red colour therefore corresponds to a three σ detection.

I noise level of 143 µK$_{RJ}$. The maps are shown in Fig. 6 along with a map of the normalized squared polarized intensity $(Q^2 + U^2)/(\sigma_Q^2 + \sigma_U^2)$. Twice this quantity is statistically distributed like a χ^2 with 2 degrees of freedom. The 68, 95.4, 99.7% CL of the mapped quantity correspond to 1.1, 3.1, 5.8 respectively.

Seven polarized Galactic dense clouds are detected at the 3σ level with sizes ranging from 2.3 to 21.6 deg^2 and polarization degree ranging from $7.5 \pm 1.7\%$ to $23.2 \pm 11\%$. The precise characteristics of these clouds are given in [23]. A search for diffuse galactic polarization shows significant (3 to 4σ) coherent polarization levels of a few percent in the Galactic plane, even after masking the dense clouds discussed above. The detected clouds appear to belong to two complexes, one in Cassiopeia that includes the CasA supernova remnant (the point source was however not projected in the maps), the other in the southern part of Gem OB1. The polarization orientation is found to be coherent between clouds and diffuse regions and nearly orthogonal to the Galactic plane. These results are in agreement with expectations from starlight polarization measurements [25], the presence of dense polarized regions provides evidence for a powerful grain alignement mechanism thoughout the interstellar medium [26] and a coherent magnetic field coplanar to the Galactic plane and following the spiral arms. Interestingly, the observed part of the Cygnus complex is not found to be significantly polarized. Projection effects along the line of sight of sight may explain the lack of detectable polarization from Cygnus region. Extrapolating these results to high Galactic latitude indicates that interstellar dust polarized emission is the major foreground for PLANCK-HFI CMB polarization measurements as suggested by [27].

8. Conclusions

Constraints on various cosmological parameters (Benoît et al. [28]) have been derived by using the Archeops data alone and in combination with other measurements. The measured power spectrum (Benoît et al. [15]) matches the Cobe data and provides for the first time a direct link between the Sachs–Wolfe plateau and the first acoustic peak, because of the large sky coverage that greatly reduces the sample variance. The measured spectrum is in good agreement with that predicted by simple inflation models of scale-free adiabatic peturbations and a flat-Λ Universe assumption. Finally let us note that these results were obtained with only half a day worth of data. Precise maps of the Galactic dust emission in the Galactic plane region have been obtained and show new sources and diffuse emission. Archeops also provides the first measurement of galactic dust polarization at 353 GHz, showing dense polarized clouds and diffuse polarization. The coherence of the polarization direction suggests the presence of a coherent magnetic field coplanar to the Galactic plane.

Use of all available bolometers and of a larger sky fraction should yield an even more accurate and broader CMB power spectrum in the near future. The large experience gained on this balloon-borne experiment is providing a large feedback to the Planck–Hfi data processing community.

References

[1] P. de Bernardis, et al., Nature 404 (2000) 995.
[2] C.B. Netterfield, et al., Astrophys. J. 571 (2002) 604.
[3] S. Hanany, et al., Astrophys. J. 545 (2000) L5.
[4] A.T. Lee, et al., Astrophys. J. 561 (2001) L1–L6.
[5] C. Pryke, et al., Astrophys. J. 568 (2002) 46.
[6] J.L. Sievers, et al., Astrophys. J., submitted for publication, astro-ph/0205387.
[7] J.A. Rubiño-Martin, et al., Mon. Not. R. Astron. Soc., submitted for publication, astro-ph/0205367.
[8] A. Benoît, et al., Astropart. Phys. 17 (2002) 101–124, astro-ph/0106152.
[9] G. Smoot, et al., Astrophys. J. Lett. 395 (1992) L1.
[10] A. Benoît, et al., in preparation.
[11] K.M. Gorski, et al., astro-ph/9812350, http://www.eso.org/science/healpix.
[12] A. Amblard, J.-Ch. Hamilton, Astron. Astrophys., submitted for publication, astro-ph/0307203.
[13] E. Hivon, et al., Astrophys. J. 567 (2002) 2.
[14] C.L. Bennett, et al., 2002, astro-ph/0302207.
[15] A. Benoît, et al., Astron. Astrophys. 399 (2003) L19, astro-ph/0210305.
[16] O'Meara, et al., Astrophys. J. 552 (2001) 718.
[17] W.L. Freedman, et al., Astrophys. J. 553 (2002) 47.
[18] M. Douspis, et al., Astron. Astrophys. 405 (2003) 409, astro-ph/0212097.
[19] S. Perlmutter, et al., Astrophys. J. 517 (2001) 565.
[20] Bøifot, et al., Proc. Inst. Elect. Eng. 137 (1990) 396.
[21] G. Chattopadhyay, et al., IEEE Microwave and Guided Wave Lett. 9 (1999) 339.
[22] F. Couchot, J. Delabrouille, J. Kaplan, B. Revenu, et al., Astron. Astrophys. Suppl. Ser. (1999) 135.
[23] A. Benoît, et al., Astron. Astrophys., submitted for publication, astro-ph/0306222.
[24] J.F. Macías-Pérez, 2003, in preparation.
[25] P. Fosalba, et al., Astrophys. J. 564 (2002) 762.
[26] R.H. Hildebrand, M. Dragovan, Astrophys. J. 450 (1995) 663.
[27] S. Prunet, et al., Astron. Astrophys. 339 (1998) 187.
[28] A. Benoît, et al., Astron. Astrophys. 399 (2003) L25, astro-ph/0210306.